Diffusion Coefficient of Naphthalene in Air and Hydrogen

Lloyd Caldwell

Chemical Engineering Research Group, Council for Scientific and Industrial Research, Pretoria 0001, Republic of South Africa

At 303.2 K and 0.1013 MPa the diffusion coefficients for naphthalene in air and hydrogen are 0.086 and 0.301 cm^2 s^{-1}, respectively, as determined with a modified Stefan tube technique in which the use of vapor pressure data and the need for accurate temperature measurements were eliminated. The standard deviation of measurements was 4.1%. The commonly accepted value for the diffusion coefficient of naphthalene in air is seriously in error, mainly because incorrect vapor pressure data were used.

Introduction

Naphthalene is a convenient solid to employ for the determination of mass-transfer coefficients in many fluid flow situations (*1-5*). It has a relatively high melting point in relation to its vapor pressure, presumably a consequence of its structural symmetry, and at room temperature it provides a reasonable compromise between the need to attain measurable rates of mass transfer and the undesirability of a too rapid change in shape or size.

In interpretation of mass-transfer results it is important that accurate data for the diffusion coefficients of the diffusing species be available. No recent determinations of the diffusion coefficient of naphthalene appear to have been made. The only published determination is Mack's (*6*) in 1925, and it is his value for naphthalene–air which is listed in Landolt-Börnstein (*7*) and (corrected for temperature) in the International Critical Tables (*8*). The review by Marrero and Mason (*9*) cites no further determinations. Based on Mack's value, the Schmidt number for dilute naphthalene–air mixtures is commonly taken as 2.57.

The work reported here was undertaken to provide a check on the value of the diffusion coefficient of naphthalene in air, and also to determine a value for the naphthalene–hydrogen system.

Method and Theory

A modification of the Stefan diffusion tube was employed. The alternative methods (*9*) are not suited to applications where one of the diffusing components is normally a solid; in particular, unsteady-state methods cannot be used at room temperature because of adsorption on the walls of the equipment. Although Marrero and Mason (*9*) criticize the Stefan technique, several of the sources of error listed by them are not found with solid–gas systems, and others may be eliminated by modification of the procedure.

For steady-state diffusion in one dimension we have (see Glossary)

$$N = \frac{FC}{a} = -D\frac{dC}{dx} = D\frac{C_0 - C}{x} \qquad (1)$$

provided that the diffusion path length, x, remains constant. This is a good approximation for diffusion from a solid surface. Hence

$$D = \frac{Fx}{a}\left(\frac{C}{C_0 - C}\right) \qquad (2)$$

The usual procedure in evaluating this expression is to obtain C_0 from vapor pressure data and to measure the total quantity sublimed (or evaporated) over a timed period; this amount, in conjunction with the measured flow rate, determines the value of C. The accuracy of the calculated value of D is thus highly dependent both on the accuracy of the vapor pressure data and on the precision of temperature measurement.

An alternative approach eliminates the need for vapor pressure data, the need to measure temperatures precisely, and also the need to make accurate weighings of the small quantities which sublime. If eq 2 is written in the form

$$C_0/C - 1 = (x/aD)F \qquad (3)$$

we see that, if C can be measured directly, then a plot of $1/C$ against F enables D to be calculated from the slope and the intercept of the resulting straight line. C can readily be measured by using a gas chromatograph detector, and, since C_0/C is merely a ratio of detector responses, there is no need to calibrate the detector provided that the response is linear over the range of interest.

A large diffusion path length (100 mm) was chosen so as to minimize end effects. In consequence, the cross-sectional area, a, had to be made large also; otherwise either the measured concentrations or the flow rates would be inconveniently small. In order to achieve a large cross section for diffusion without introducing convection effects, a multitube diffusion cell was constructed.

Equipment and Procedure

The diffusion cell is shown in Figure 1. Construction was of brass to provide good heat transfer. Fifty-two tubes of 5.48-mm bore and 100-mm length were soldered on a square pitch into end plates of 70-mm diameter. The whole assembly was sealed into a cylindrical shell. Caps with O-ring seals were screwed onto both ends of the shell to provide an upper and a lower chamber connected solely through the tubes. The lower chamber consisted of a circular recess of depth 3 mm in the upper face of the cap. This recess was filled with a slab of cast naphthalene which butted precisely against the lower tube plate. The naphthalene was BDH, "for molecular weight determinations", melting point 353.3–353.4 K. The upper chamber was provided with gas inlet and outlet connections.

In operation the cell was totally immersed in a water bath at 303.2 K and a steady flow of air or hydrogen passed through the upper chamber. A manometer measured the pressure immediately upstream of the cell. Exit gas from the cell passed through a heated line to a 0.5-cm^3 gas sample valve loop; gas samples were analyzed with a single flame ionization detector (FID). Carrier gas to the detector was the same as the gas flowing to the diffusion cell and no chromatographic column was necessary. The sample valve and line to the detector were held at 523.2 K.

After the gas flow rate to the cell was set, approximately 40 min was allowed for the attainment of steady-state conditions. The criterion for steady state was the constancy of gas sample concentrations over a 15-min period. Gas flow rate to the cell was measured by using displacement of water (first saturated with gas) from a standard volumetric flask and making allowance for water vapor pressure. A set of five gas samples was analyzed and the mean response of the detector recorded, provided that the standard deviation did not exceed 5%. Gas

0021-9568/84/1729-0060$01.50/0

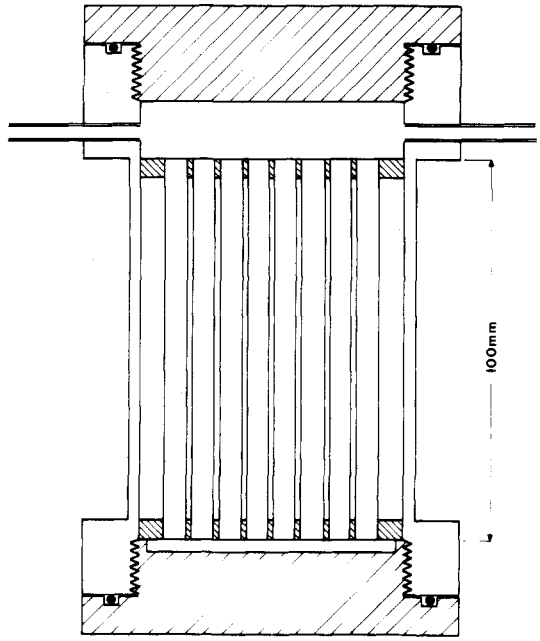

Figure 1. Diffusion cell. There are 52 tubes of total cross-sectional area 12.26 cm^2.

flow rate was then measured again; flow variations did not exceed 0.5%.

A series of such determinations was made for different gas flow rates: these varied from 0.08 to 0.4 $cm^3\ s^{-1}$ in the case of air and from 0.2 to 1.0 $cm^3\ s^{-1}$ for hydrogen. An additional point on the graph of reciprocal detector response against flow rate was provided by replacing the diffusion cell with a tube packed with naphthalene pellets. This gave the saturation response and hence was equivalent to the response from the diffusion cell at zero flow. A check was made that varying the flow rate to the packed tube did not affect the detector response.

Results

Figure 2 shows the plot of one of a set of three determinations made for naphthalene–air. The points closely approximate a straight line, although there is an indication (also seen in the other determinations) that at the highest flow rate the detector response is greater than it should be. This may be owing to a stirring effect at the end of the diffusion tubes at high flow rates.

The mean of three determinations gave the diffusion coefficient for naphthalene in air as 0.086 $cm^2\ s^{-1}$ at 303.2 K and 0.1013 MPa (1 atm), with a standard deviation of 4.1%. For both air and hydrogen the measured diffusion coefficients have been corrected to atmospheric pressure by assuming a reciprocal dependence. Measured pressures were approximately 0.0906 MPa.

Figure 3 shows the single determination made for naphthalene–hydrogen. The plot is not linear, presumably because of the higher gas flow rates which had to be employed to cover the same range of detector responses as with air. In the calculation of the diffusion coefficient the slope of the line through the first two points only was used. A value of 0.301 $cm^2\ s^{-1}$ was obtained for the diffusion coefficient at 303.2 K and 0.1013 MPa.

Discussion

A potential source of systematic error in the technique described here is nonuniformity of concentration in the upper chamber of the diffusion cell. Some degree of mixing must, of course, be introduced by the inflow of gas, and the linearity of

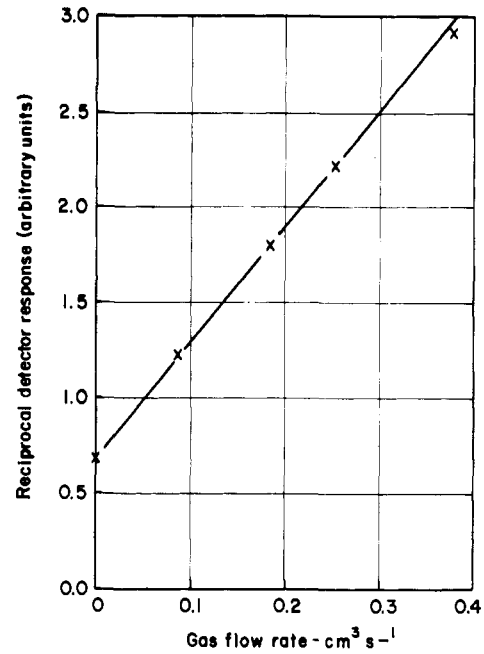

Figure 2. Typical results for naphthalene in air at 303.2 K and 0.0906 MPa.

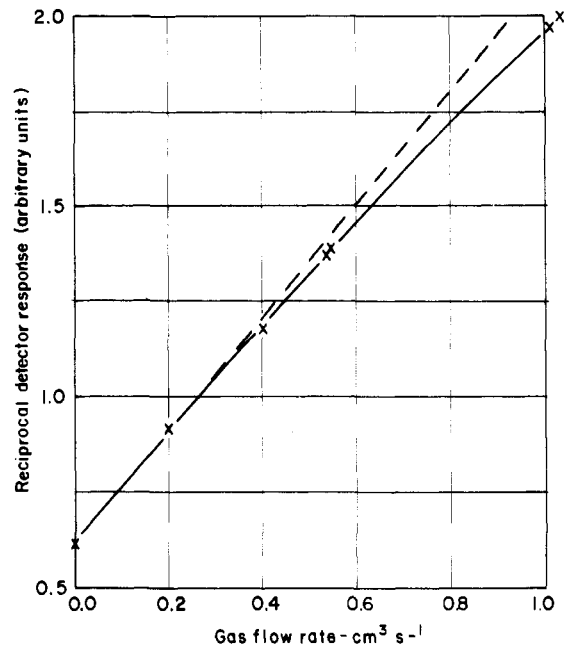

Figure 3. Naphthalene in hydrogen at 303.2 K and 0.0906 MPa.

the plots suggests that mixing is good. It would be possible to ensure good mixing by the installation of a low-speed stirrer, but this might also create disturbances in the diffusion tubes. There are clear indications that disturbances occur at gas flows greater than 0.4 $cm^3\ s^{-1}$.

The value of the diffusion coefficient for naphthalene–air is markedly higher than Mack's value of 0.0611 $cm^2\ s^{-1}$ at 298.2 K and 0.1013 MPa.

There are two sources of error in Mack's result. In the first place his calculations (not only for naphthalene but also for other substances) are not very accurate. Calculating correctly, he should have obtained a value of 0.0621 $cm^2\ s^{-1}$ for naphthalene. More importantly, Mack has used the vapor pressure data of Barker (*10*) and these differ considerably from more recent (and consistent) determinations (*11*, *12*). According to Bradley and Cleasby (*11*), the vapor pressure of naphthalene at 298.2 K is 10.86 Pa as opposed to the figure of 13.73 Pa (0.103 mmHg) used by Mack. Making this additional correction,

Mack's determination would yield $D_{298.2\ K} = 0.0786\ cm^2\ s^{-1}$, or $D_{303.2\ K} = 0.0810\ cm^2\ s^{-1}$ if we take the exponent for the temperature correction (*13*) as 1.81. This figure differs from the present determination by 6.2%.

From the data presented here the Schmidt numbers for dilute naphthalene–air and naphthalene–hydrogen mixtures are calculated to be 1.805 and 3.65, respectively.

Glossary

a	cross-sectional area for diffusion, cm^2
C	concentration of diffusing species in gas stream leaving diffusion cell, mol cm^{-3}
C_0	concentration of diffusing species at the initial end of the diffusion path, mol cm^{-3}
D	diffusion coefficient, $cm^2\ s^{-1}$
F	gas flow rate, $cm^3\ s^{-1}$
N	flux of diffusing species, mol $cm^{-2}\ s^{-1}$
x	length of diffusion path, cm

Registry No. Naphthalene, 91-20-3; hydrogen, 1333-74-0.

Literature Cited

(1) Winding, C. C.; Cheney, A. J. *Ind. Eng. Chem.* **1948**, *40*, 1067.
(2) Macleod, N.; Cox, M. D.; Todd, R. B. *Chem. Eng. Sci.* **1982**, *17*, 923.
(3) Bar-Ilan, M.; Resnick, W. *Ind. Eng. Chem.* **1957**, *49*, 313.
(4) Hurt, D. M. *Ind. Eng. Chem.* **1943**, *35*, 522.
(5) Caldwell, L. *Appl. Catal.* **1982**, *4*, 13.
(6) Mack, E. *J. Am. Chem. Soc.* **1925**, *47*, 2468.
(7) Landolt-Börnstein. "Zahlenwerte und Funktionen aus Physik, Chemie, Astronomie, Geophysik und Technik"; 6ste Auflage, II Band, 5 Teil, Springer-Verlag: West Berlin, 1969; p 553.
(8) "International Critical Tables"; McGraw-Hill: New York, 1929; Vol. 5, p 63.
(9) Marrero, T. R.; Mason, E. A. *J. Phys. Chem. Ref. Data* **1972**, *1*, 3.
(10) Barker, J. T. *Z. Phys. Chem.* **1910**, *71*, 235.
(11) Bradley, R. S.; Cleasby, T. G. *J. Chem. Soc.* **1953**, 1690.
(12) Skelland, A. H. P. "Diffusional Mass Transfer"; Wiley: New York, 1974; p 118.
(13) Chen, N. H.; Othmer, D. F. *J. Chem. Eng. Data* **1962**, *7*, 37.

Received for review March 22, 1983. Accepted August 1, 1983.

Acridine Orange Association Equilibrium in Aqueous Solution

Lucia Costantino, Gennaro Guarino, Ornella Ortona, and Vincenzo Vitagliano*

Instituto Chimico Università di Napoli, Naples, Italy

An accurate set of absorption spectra in the visible region has been collected for acridine orange (AO) hydrochloride in aqueous solution at various temperatures and concentrations. The limiting extinction spectra of monomer, dimer, and associated dye species were computed from the experimental data. The free energy, enthalpy, and entropy of dye dimerization have also been computed.

Introduction

Acridine orange (AO) behavior in aqueous solution and its interaction with synthetic and biological polyelectrolytes have been the subject of a very wide literature for 30 years (*1*).

The reason for the interest in AO and similar dyes is mainly connected with their ability to interact with genetic material (*2*, *3*); the similarity of these molecules to several antibiotics, such as daunomycin or actinomycin (*4*), makes them interesting model systems for studying a variety of bio- and physicochemical problems.

AO is a cationic dye, it is protonated at a pH lower than 10–10.5, and its spectrum does not agree with Beer's law. Figure 1 shows the extinction spectra in the visible region of acridine orange hydrochloride in aqueous solution, in the concentration range 10^{-5}–10^{-1} mol/L.

The absorption spectrum of dilute AO, having a maximum at 492 nm (α band), is gradually substituted by a new spectrum with a maximum at 465 nm (β band). In the concentration range below (4–5) × 10^{-5} mol/L an isosbestic point is observed at 471.5 nm.

At higher concentrations the 465-nm band is substituted by a third band (γ band) with a maximum at 450 nm and the isosbestic point disappears.

Such a behavior, characteristic of all metachromatic dyes (acridine derivatives, methylene blue, crystal violet, cyanine dyes, etc.), has been interpreted as due to the association of dye molecules in solution (*1*, *5*).

We have recently studied the association for several *N*-alkyl derivatives of acridine orange and computed the dimerization constants and other thermodynamic properties to compare them with those of AO available in the literature (*6*, *7*).

At this point we thought it convenient to collect a new set of experimental absorption data on AO aqueous solutions in the full range of possible dye concentrations and decided to treat them like those of the other acridine dyes, in order to have a full set of self-consistent thermodynamic data, including the first molecule of the series.

The results discussed in the following were obtained from the analysis of about 200 spectra taken at various concentrations and temperatures.

The association, or stacking, of dye molecules in solution, promoted by the π-electron interactions of aromatic rings, can be described as a set of multiple equilibria of the following type:

$$D + D = D_2 \quad (1)$$

$$D_2 + D = D_3 \quad (2)$$

...

$$D_{n-1} + D = D_n \quad (3)$$

It may be assumed that dye molecules stack in a sandwichlike pile. The α absorption band was attributed to the dye in its monomeric form, the β band to the dimer dye, and the γ band to dye in a higher associated form.

The observed spectral changes have also been predicted theoretically for an association according to this model (*8*, *9*).

The equilibrium constants for the associations 1–3 are given by the following expressions:

$$[D_2] = K_{12}[D]^2 \quad (4)$$

$$[D_3] = K_{12}K_{23}[D]^3 \quad (5)$$

...

$$[D_n] = K_{12}K_{23}...K_{n-1,n}[D]^n \quad (6)$$

0021-9568/84/1729-0062$01.50/0